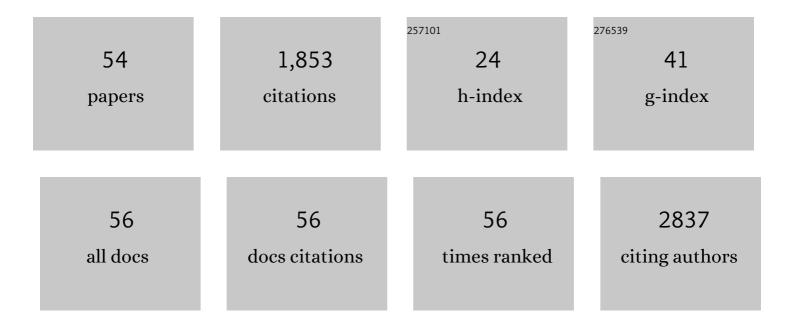
Xiaoshuang Zhou

List of Publications by Year in descending order

Source: https://exaly.com/author-pdf/6707819/publications.pdf Version: 2024-02-01



#	Article	IF	CITATIONS
1	Design of an Inorganic Mesoporous Holeâ€Transporting Layer for Highly Efficient and Stable Inverted Perovskite Solar Cells. Advanced Materials, 2018, 30, e1805660.	11.1	179
2	Downsized Sheath–Core Conducting Fibers for Weavable Superelastic Wires, Biosensors, Supercapacitors, and Strain Sensors. Advanced Materials, 2016, 28, 4998-5007.	11.1	131
3	Unipolar stroke, electroosmotic pump carbon nanotube yarn muscles. Science, 2021, 371, 494-498.	6.0	110
4	Temperature-independent capacitance of carbon-based supercapacitor from â^'100 to 60 °C. Energy Storage Materials, 2019, 22, 323-329.	9.5	104
5	A Biâ€Sheath Fiber Sensor for Giant Tensile and Torsional Displacements. Advanced Functional Materials, 2017, 27, 1702134.	7.8	100
6	Defect mitigation using <scp>d</scp> -penicillamine for efficient methylammonium-free perovskite solar cells with high operational stability. Chemical Science, 2021, 12, 2050-2059.	3.7	88
7	Enhanced rate performance of flexible and stretchable linear supercapacitors based on polyaniline@Au@carbon nanotube with ultrafast axial electron transport. Journal of Power Sources, 2017, 340, 302-308.	4.0	67
8	Heterojunction Engineering for High Efficiency Cesium Formamidinium Double ation Lead Halide Perovskite Solar Cells. ChemSusChem, 2018, 11, 837-842.	3.6	61
9	High Efficiency Planar pâ€iâ€n Perovskite Solar Cells Using Lowâ€Cost Fluoreneâ€Based Hole Transporting Material. Advanced Functional Materials, 2019, 29, 1900484.	7.8	59
10	Dibenzo[<i>b</i> , <i>d</i>]thiopheneâ€Cored Holeâ€Transport Material with Passivation Effect Enabling the Highâ€Efficiency Planar p–i–n Perovskite Solar Cells with 83% Fill Factor. Solar Rrl, 2020, 4, 1900421.	3.1	47
11	Crystallization tailoring of cesium/formamidinium double-cation perovskite for efficient and highly stable solar cells. Journal of Energy Chemistry, 2020, 48, 217-225.	7.1	45
12	Robust ZIF-8/alginate fibers for the durable and highly effective antibacterial textiles. Colloids and Surfaces B: Biointerfaces, 2020, 193, 111127.	2.5	42
13	Ultraflexible and Lightweight Bambooâ€Derived Transparent Electrodes for Perovskite Solar Cells. Small, 2019, 15, e1902878.	5.2	40
14	Activated carbon coated CNT core-shell nanocomposite for supercapacitor electrode with excellent rate performance at low temperature. Electrochimica Acta, 2019, 301, 478-486.	2.6	40
15	A self-healing conductive and stretchable aligned carbon nanotube/hydrogel composite with a sandwich structure. Nanoscale, 2018, 10, 19360-19366.	2.8	39
16	Interfacial Contact Passivation for Efficient and Stable Cesium-Formamidinium Double-Cation Lead Halide Perovskite Solar Cells. IScience, 2020, 23, 100762.	1.9	37
17	Nano-structured red phosphorus/porous carbon as a superior anode for lithium and sodium-ion batteries. Science China Materials, 2018, 61, 371-381.	3.5	35
18	Improve the electrodeposition of sulfur and lithium sulfide in lithium-sulfur batteries with a comb-like ion-conductive organo-polysulfide polymer binder. Energy Storage Materials, 2019, 18, 190-198.	9.5	35

XIAOSHUANG ZHOU

#	Article	IF	CITATIONS
19	Hierarchical Porous Carbon Arising from Metal–Organic Framework-Encapsulated Bacteria and Its Energy Storage Potential. ACS Applied Materials & Interfaces, 2020, 12, 11884-11889.	4.0	33
20	Graphene-based fibers for the energy devices application: A comprehensive review. Materials and Design, 2021, 201, 109476.	3.3	32
21	Low temperature tolerant, ultrasensitive strain sensors based on self-healing hydrogel for self-monitor of human motion. Synthetic Metals, 2019, 257, 116177.	2.1	30
22	<i>N</i> , <i>N</i> -Di- <i>para</i> -methylthiophenylamine-Substituted (2-Ethylhexyl)-9 <i>H</i> -Carbazole: A Simple, Dopant-Free Hole-Transporting Material for Planar Perovskite Solar Cells. Journal of Physical Chemistry C, 2017, 121, 21821-21826.	1.5	29
23	Visual and flexible temperature sensor based on a pectin-xanthan gum blend film. Organic Electronics, 2018, 59, 243-246.	1.4	28
24	Highly stretchable CNT/MnO2 nanosheets fiber supercapacitors with high energy density. Journal of Materials Science, 2020, 55, 8251-8263.	1.7	27
25	Self-healing hydrogel sensors with multiple shape memory properties for human motion monitoring. New Journal of Chemistry, 2021, 45, 314-320.	1.4	25
26	Fluorinating Dopant-Free Small-Molecule Hole-Transport Material to Enhance the Photovoltaic Property. ACS Applied Materials & amp; Interfaces, 2021, 13, 7705-7713.	4.0	25
27	A High Stretchable and Self–Healing Silicone Rubber with Double Reversible Bonds. ChemistrySelect, 2019, 4, 10719-10725.	0.7	23
28	Superior Textured Film and Process Tolerance Enabled by Intermediateâ€State Engineering for Highâ€Efficiency Perovskite Solar Cells. Advanced Science, 2020, 7, 1903009.	5.6	22
29	Unimpeded migration of ions in carbon electrodes with bimodal pores at an ultralow temperature of â~'100 °C. Journal of Materials Chemistry A, 2019, 7, 16339-16346.	5.2	21
30	Fast Largeâ€Stroke Sheathâ€Driven Electrothermal Artificial Muscles with High Power Densities. Advanced Functional Materials, 2022, 32, .	7.8	21
31	A transparent, tough self-healing hydrogel based on a dual physically and chemically triple crosslinked network. Journal of Materials Chemistry C, 2019, 7, 14581-14587.	2.7	20
32	Excellent Rate and Low Temperature Performance of Lithiumâ€ion Batteries based on Binderâ€Free Li 4 Ti 5 O 12 Electrode. ChemElectroChem, 2020, 7, 716-722.	1.7	19
33	Interfacial passivation of wide-bandgap perovskite solar cells and tandem solar cells. Journal of Materials Chemistry A, 2021, 9, 21939-21947.	5.2	19
34	Sunlight-Driven Continuous Flapping-Wing Motion. ACS Applied Materials & Interfaces, 2020, 12, 6460-6470.	4.0	18
35	A multifunctional zipper-like sulfur electrode enables the stable operation of lithium-sulfur battery through self-healing chemistry. Energy Storage Materials, 2021, 34, 755-767.	9.5	18
36	Stable High-Performance Perovskite Solar Cells via Passivation of the Grain Boundary and Interface. ACS Applied Energy Materials, 2021, 4, 6883-6891.	2.5	18

XIAOSHUANG ZHOU

#	Article	IF	CITATIONS
37	O,N-Codoped 3D graphene hollow sphere derived from metal–organic frameworks as oxygen reduction reaction electrocatalysts for Zn-air batteries. Nanoscale, 2021, 13, 6174-6183.	2.8	17
38	Self-Healing Silicone Elastomer with Stable and High Adhesion in Harsh Environments. Langmuir, 2021, 37, 13696-13702.	1.6	17
39	Carbon Nanotube Hybrid Yarn with Mechanically Strong Healable Silicone Elastomers for Artificial Muscle. ACS Applied Nano Materials, 2021, 4, 5123-5130.	2.4	16
40	cells: insight into the carrier ultrafast dynamics and interfacial transport. Science China Chemistry, 2020, 63, 827-832.	4.2	13
41	Oxygen-tailoring in SiO _{<i>X</i>} /C with a covalent interface for high-performance lithium storage. Journal of Materials Chemistry A, 2022, 10, 1928-1939.	5.2	13
42	3D TM-N-C Electrocatalysts with Dense Active Sites for the Membraneless Direct Methanol Fuel Cell and Zn-Air Batteries. Langmuir, 2022, 38, 4948-4957.	1.6	10
43	A new laminated structure for electrodes to boost the rate performance of long linear supercapacitors. Materials Letters, 2017, 204, 177-180.	1.3	8
44	Wire‧haped and Membraneâ€Free Fuel Cell Based on Biscrolled Carbon Nanotube Yarn. Energy Technology, 2019, 7, 1900122.	1.8	8
45	Electrical energy generation by squeezing a graphene-based aerogel in an electrolyte. Nanoscale, 2021, 13, 8304-8312.	2.8	8
46	Graphene Oxide Aerogel Foam Constructed All-Solid Electrolyte Membranes for Lithium Batteries. Langmuir, 2022, 38, 3257-3264.	1.6	8
47	Miniaturized Stretchable and High-Rate Linear Supercapacitors. Nanoscale Research Letters, 2017, 12, 448.	3.1	7
48	Evaluating the interfacial properties of wrinkled graphene fiber through single-fiber fragmentation tests. Journal of Materials Science, 2020, 55, 1023-1034.	1.7	7
49	A highly sensitive piezoresistive sensor based on CNT-rGO aerogel for human motion detection. Journal of Composite Materials, 2021, 55, 3661-3669.	1.2	7
50	Conducting Fibers: Downsized Sheath–Core Conducting Fibers for Weavable Superelastic Wires, Biosensors, Supercapacitors, and Strain Sensors (Adv. Mater. 25/2016). Advanced Materials, 2016, 28, 4946-4946.	11.1	6
51	Fast polysulfide catalytic conversion and self-repairing ability for high loading lithium–sulfur batteries using a permselective coating layer modified separator. Nanoscale, 2021, 13, 17592-17602.	2.8	5
52	N-Doped graphene supported on N-rGO nanosheets as metal-free oxygen reduction reaction electrocatalysts for Zn–air batteries. New Journal of Chemistry, 2021, 45, 21716-21724.	1.4	5
53	Flexible Actuator and Generator Stimulated by Organic Vapors. Journal of Inorganic and Organometallic Polymers and Materials, 2018, 28, 1962-1967.	1.9	4
54	A wide-temperature-range sensor based on wide-strain-range self-healing and adhesive organogels. New Journal of Chemistry, 2022, 46, 4334-4342.	1.4	4